



ELSEVIER

Contents lists available at ScienceDirect

## Science Bulletin

journal homepage: [www.elsevier.com/locate/scib](http://www.elsevier.com/locate/scib)Science  
Bulletin[www.scibull.com](http://www.scibull.com)

## Article

# A systematic survey of PRMT interactomes reveals the key roles of arginine methylation in the global control of RNA splicing and translation

Huan-Huan Wei <sup>a,\*</sup>, Xiao-Juan Fan <sup>a</sup>, Yue Hu <sup>a</sup>, Xiao-Xu Tian <sup>b</sup>, Meng Guo <sup>a,c</sup>, Miao-Wei Mao <sup>a</sup>, Zhao-Yuan Fang <sup>a</sup>, Ping Wu <sup>b</sup>, Shuai-Xin Gao <sup>b</sup>, Chao Peng <sup>b</sup>, Yun Yang <sup>a</sup>, Zefeng Wang <sup>a,\*</sup>

<sup>a</sup> CAS Key Laboratory of Computational Biology, Bio-Med Big Data Center, Shanghai Institute of Nutrition and Health, CAS Center for Excellence in Molecular Cell Science, University of Chinese Academy of Sciences, Chinese Academy of Sciences, Shanghai 200031, China

<sup>b</sup> National Facility for Protein Science in Shanghai, Zhang-Jiang Lab, Shanghai Advanced Research Institute, Chinese Academy of Sciences, Shanghai 201210, China

<sup>c</sup> Xijing Hospital of Digestive Diseases, Fourth Military Medical University, Xi'an 710000, China

## ARTICLE INFO

## Article history:

Received 17 July 2020

Received in revised form 13 October 2020

Accepted 30 December 2020

Available online xxxx

## Keywords:

Post-translational modification  
Protein arginine methyltransferase  
RNA-binding protein  
Ribosomal proteins  
Alternative splicing  
mRNA translation

## ABSTRACT

Thousands of proteins undergo arginine methylation, a widespread post-translational modification catalyzed by several protein arginine methyltransferases (PRMTs). However, global understanding of their biological functions is limited due to the lack of a complete picture of the catalytic network for each PRMT. Here, we systematically identified interacting proteins for all human PRMTs and demonstrated their functional importance in mRNA splicing and translation. We demonstrated significant overlapping of interactomes of human PRMTs with the known methylarginine-containing proteins. Different PRMTs are functionally redundant with a high degree of overlap in their substrates and high similarities between their putative methylation motifs. Importantly, RNA-binding proteins involved in regulating RNA splicing and translation contain highly enriched arginine methylation regions. Moreover, inhibition of PRMTs globally alternates alternative splicing (AS) and suppresses translation. In particular, ribosomal proteins are extensively modified with methylarginine, and mutations in their methylation sites suppress ribosome assembly, translation, and eventually cell growth. Collectively, our study provides a global view of different PRMT networks and uncovers critical functions of arginine methylation in regulating mRNA splicing and translation.

© 2021 Science China Press. Published by Elsevier B.V. and Science China Press. This is an open access article under the CC BY-NC-ND license (<http://creativecommons.org/licenses/by-nc-nd/4.0/>).

## 1. Introduction

Arginine N-methylation is catalyzed by a class of enzymes known as protein arginine methyltransferases (PRMTs) that covalently link methyl groups to arginine side chains. It was first discovered in the early 1970s [1–3] and subsequently recognized as a widespread post-translational modification (PTM) of proteins [4–9]. Although arginine methylation does not alter the electric charge, it increases the amino acid bulkiness and protein hydrophobicity, thereby regulating how proteins interact with their partners. Arginine methylation participates in several cellular processes, including phase separation, DNA damage repair, transcriptional regulation, and RNA metabolism [6–13]. Thus, arginine

methylation has a profound effect on human diseases such as cancer [9,14,15] and cardiovascular diseases [16].

Nine PRMTs, PRMT1 to PRMT9, have been identified in the human genome (Fig. 1a), which are further classified into three types according to the final methylarginine products. Type I PRMTs, including PRMT1, 2, 3, 4, 6, and 8, catalyze the formation of  $\omega$ -N<sup>G</sup>, N<sup>G</sup>-asymmetric dimethylarginine (aDMA). Type II PRMTs, including PRMT5 and PRMT9, catalyze the formation of  $\omega$ -N<sup>G</sup>, N<sup>G</sup>-symmetric dimethylarginine (sDMA). PRMT7 is the only type III PRMT and catalyzes the formation of  $\omega$ -N<sup>G</sup>-monomethylarginine (MMA). Although the methyltransferase domain is highly conserved across the nine PRMTs, certain PRMTs have additional less conserved motifs to regulate their stability and functions (Fig. 1a). Methylation of arginine by PRMTs is a highly energy-consuming process (12 ATPs for each methyl group added) [4] and is found in more than 10% of all human proteins [17], implying an essential role of arginine methylation in cell growth and proliferation.

\* Corresponding authors.

E-mail addresses: [weihuanhuan@picb.ac.cn](mailto:weihuanhuan@picb.ac.cn) (H.-H. Wei), [wangzefeng@picb.ac.cn](mailto:wangzefeng@picb.ac.cn) (Z. Wang).

The biological functions of PRMTs are largely determined by their substrates and regulating partners. Therefore, identifying the full scope of interactors for each PRMT will greatly improve our understanding of the functional significance of arginine methylation. The substrates of several individual PRMTs (e.g., PRMT4 and PRMT5) have been determined using multiple approaches [18–20], however, the substrates or interactors of other PRMTs remain largely unknown. Besides, thousands of human proteins have been identified to undergo arginine methylation using a combination of mass spectrometry and specific anti-methylarginine antibodies [17,21]. Therefore, efforts to connect these arginine-methylated proteins with their respective PRMTs are highly valuable to further understand their regulation and functions.

In this study, we systematically identified the interactome of each PRMT using the BioID methods [22–24] and mass spectrometry (MS), then further determined the substrate specificity and consensus arginine methylation motifs of each PRMT. Our results revealed a high degree of overlap in the substrate specificity of different PRMTs, suggesting a possible functional redundancy. Remarkably, PRMT interactors were significantly enriched for RNA binding proteins involved in mRNA splicing and translation. Inhibition of PRMTs globally altered alternative splicing and reduced mRNA translation. Particularly, mutations in the methylation sites of ribosomal proteins inhibited ribosome assembly and cell growth. Thus, our study systematically linked individual PRMTs to their arginine methylation events and highlighted their importance in regulating RNA metabolism.

## 2. Materials and methods

### 2.1. Plasmids

For identifying the interacting proteins of each PRMT, human PRMT1–PRMT9 were amplified by PCR and inserted into the pcDNA3.1-BirA-HA plasmid (#36047, Addgene, Watertown, USA). For *in vitro* methylation, Myc-tagged PRMTs (PRMT1 to PRMT9) were inserted into pcDNA3.1-Myc-tag plasmids. For ribosome assembly, Myc-tagged hRPS2 was generated by PCR from human cDNA and inserted into the frame with pcDNA3.1-Myc. The RPS2 mutants with arginine to alanine or lysine substitution (R22/26/34/36/227/279A, 6RA, and R22/26/34/36/227/279 K, 6RK) were generated by site-directed mutagenesis.

### 2.2. Identification of interacting proteins for each PRMT

Human PRMT1–PRMT9 were amplified by PCR and inserted into the pcDNA3.1-BirA plasmid. The BioID experiments were performed as described by Roux et al. [24] with minor modifications. Briefly, HEK293T cells transiently expressing PRMT-BirA fusion proteins were collected and lysed. The protein complexes were purified using streptavidin beads. The resulting protein mixture was further separated by high-performance liquid chromatography (HPLC) using a custom 15 cm-long, pulled-tip analytical column, and analyzed using mass spectrometry. The acquired MS/MS data were compared to the UniProt database using the Integrated Proteomics Pipeline. A decoy database containing the reversed sequences of all proteins was appended to the target database to accurately estimate peptide probabilities and false discovery rate (FDR, set at 0.01).

Three biological replicates were performed for mock control and each PRMT individually. The label-free quantification (LFQ) of proteins was performed using the built-in algorithm maxLFQ with the “delayed normalization” option [25]. Only proteins with at least two valid LFQ intensity values in three replicates (Table S1 online) were considered and the average intensity was

subsequently calculated. We identified putative interactors of each PRMT by evaluating protein quantification values of all proteins and scored the positive hits using an LFQ intensity cutoff of two-fold higher than that in the mock control.

### 2.3. Motif enrichment analysis

We retrieved the full sequences of all identified interactors of each PRMT from the UniProt database (2019\_11, <https://www.uniprot.org/>). We counted all tetrapeptides with arginine amino acid at each position (candidate PRMT's binding sites) and calculated the frequency of each tetrapeptide in each PRMT interactome. We next compared it with the background tetrapeptide frequency of all human proteins from the UniProt database. The enrichment score of each tetrapeptide was calculated as a Z score, as previously described [26]. We collected all motifs with an enrichment score of more than 4 and motif number more than 6 as an input of Clustal-w2 (v2.0.9, <https://www.ebi.ac.uk/Tools/msa/clustalw2/>) to generate hierarchical dendograms. Next, we clustered these motifs based on branch length and modified them manually to ensure similar motifs in one class. Finally, we used Weblogo3 (<http://weblogo.berkeley.edu/>) to draw the consensus sequence of each cluster.

### 2.4. *In vitro* methylation and MS detection of arginine methylated peptides

The HEK293T cells transiently overexpressing Myc-tagged PRMT were lysed, and the overexpressed proteins were purified using anti-Myc magnetic beads (Pierce, Hallsboro, USA). *In vitro* methylation assay was performed as described by Cheng et al. [27] with minor modifications. Peptide substrates containing predicted motifs and recombinant enzyme (on beads) were incubated in the presence of S-adenosyl-L-methionine (AdoMet, Sigma, St. Louis, USA). The reaction mixture was further separated by HPLC using a custom analytical column and analyzed using mass spectrometry. The acquired MS/MS data were analyzed on a custom database, including all target peptides using PEAKS Studio (version 8.5, Thermo Scientific, Waltham, USA). Monomethylation and dimethylation were set as dynamic modifications with mass shifts at 14.01565 and 28.0313, respectively. For each peptide, the sum of the peak areas from the total ion current (TIC) values of the modified peptides was divided by the peak area of the total peptides. This value was used as a relative index of the methylation percentage.

### 2.5. Generation of stable cell lines

Lentivirus particles were constructed according to the Addgene pLKO.1 protocol. Scrambled shRNA and PRMT shRNA sequences are listed in Table S3 (online). Lentiviruses were packaged by transfection of three plasmids (pLKO.1, psPAX2, and pMD2.G.) into HEK293T cells. The stably transfected cells were selected with puromycin for at least two weeks. The knockdown efficiency was determined by anti-PRMT antibodies.

### 2.6. RNA-seq

HEK293T cells stably transfected with scrambled shRNA or shRNAs against PRMT were harvested in the Trizol reagent. RNAs were extracted according to the manufacturer's protocol. Poly (A) + RNA-seq libraries were prepared using the Illumina TruSeq Stranded mRNA LT Sample Prep Kit (Illumina, San Diego, USA) and subjected to deep sequencing with Illumina HiSeq X10 under the PE150 sequencing model.

## 2.7. Immunoprecipitation and substrate validation

The HEK293T lysate was separated into three parts that were incubated with anti-ADme-, SDme-, and Mme-arginine antibodies, respectively. The A/G PLUS-Agarose beads (Santa Cruz, Santa Cruz, USA) were used to immunoprecipitate methylarginine-containing substrates. The candidate substrates (ribosomal proteins) were detected by Western blotting.

## 2.8. Polysome profiling

Polysome profiling was performed according to established protocols [28,29]. HEK293T cells treated with PRMT1 and PRMT1 inhibitors as well as PRMT1 or PRMT4 knockdown stable cell lines were lysed in the polysome lysis buffer. The lysates were loaded onto 10% to 50% sucrose gradients and ultracentrifuged. Fractions were collected using a Brandel (Gaithersburg, USA) density gradient fractionation system. Protein samples could either be precipitated with methanol/chloroform method according to the sucrose gradient separation protocol (<http://www.mitosciences.com/PDF/sq.pdf>) or directly analyzed by Western blotting. The protein precipitate was assayed by Western blotting to detect arginine methylation status using indicated antibodies (antibodies are listed in Table S3 online).

## 2.9. RNA-seq of polysome profiling fractions

The mRNAs from indicated fractions of polysome profiling samples were extracted with the Trizol reagent. The RNA-seq libraries were prepared by NEBNext® EULtra™ II Directional RNA Library Prep Kit for Illumina (NEB, Ipswich, USA) and subjected to deep sequencing with Illumina HiSeq X10 under the PE150 sequencing model.

## 2.10. Measurement of global protein synthesis by puromycin incorporation

HEK293T, U2OS, or PC9 cells were incubated with specific inhibitors (Table S3 online) against several PRMTs. Subsequently, the puromycin incorporation assay was performed according to the method described by Kelleher et al. [30]. Puromycin was added to the medium of inhibitor-treated cells 30 min before harvest. An equal quantity of protein lysates was separated on SDS/PAGE and probed with an anti-puromycin antibody (Millipore, Burlington, USA).

## 2.11. Ribosome footprint

Cleared cell lysates from polysome profiling were treated with RNase I to obtain ribosome-protected mRNA fragments (RPFs). Subsequently, lysates were loaded onto 10% to 50% sucrose gradients, ultracentrifuged, and fractionated as described above. Fractions containing the monoribosome particles were combined and subjected to RNA clean-up using the Trizol reagent. The RNA sequencing library was prepared according to the method described by Ingolia et al. [31] with slight modifications. The RPF library was constructed as described in the Illumina Small RNA Library Prep Reference Guide. RNA samples were reverse-transcribed and cDNA libraries were gel purified and amplified by limited-cycle PCR with index primers. Libraries were cleaned up and subjected to next-generation sequencing on Illumina HiSeq X10.

## 2.12. Bioinformatics analyses

The R package GeneOverlap was used to assess the significance of substrate overlap between different PRMTs, with the total number of interacting proteins identified as the background. Gene

ontology (GO) analysis of putative PRMT substrates was performed using Database for Annotation, Visualization and Integrated Discovery (DAVID, v6.8, <https://david.ncifcrf.gov/home.jsp>), with the total proteins in the human genome as the background. Protein-protein interactions were obtained from the STRING database [32] with interaction score set to high confidence, subsequently clustered, [33] and demonstrated in Gephi (<https://gephi.org/>).

For analysis of alternative splicing, the RNA-seq reads were mapped onto the human genome reference (Ensembl GRCh37, <https://ensembl.org>), and the percent spliced in (PSI) values were estimated using MISO (v0.5.4, <https://miso.readthedocs.io/en/fatmiso/>) and rMATs (v4.0.2, <https://github.com/Xinglab/rmats-turbo>) for each annotated splicing event. The significance of splicing change was filtered using an FDR cutoff of 0.01. We also used a ΔPSI cutoff of 0.1 with a minimal read count at 50.

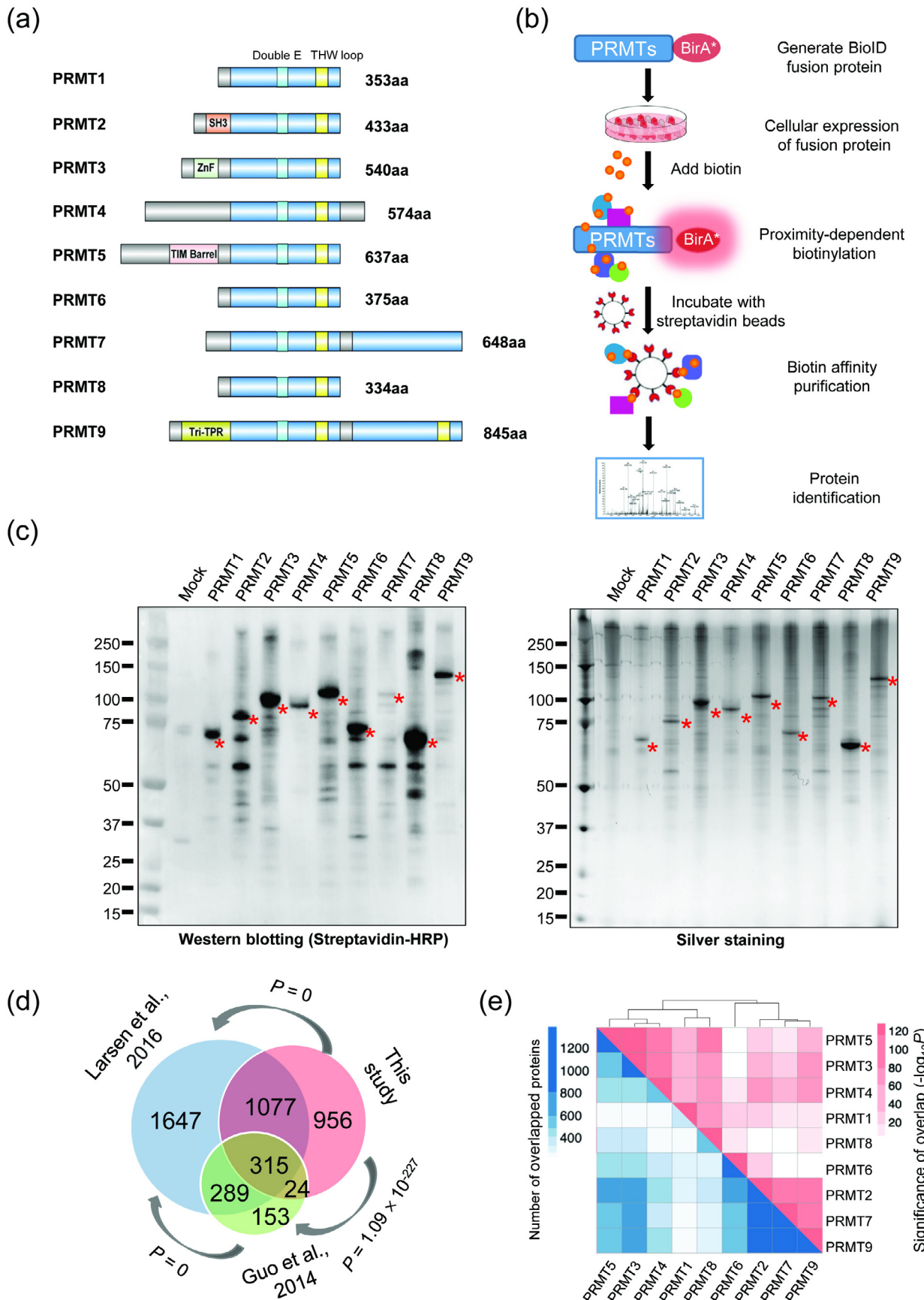
To analyze RNA-seq data following polysome profiling, we trimmed the adaptors and low-quality bases of paired-end 150 bp reads using Cutadapt (v1.18, <https://cutadapt.readthedocs.io/en/stable/>). The trimmed reads with length less than 20 nucleotides were excluded, and the remaining reads were mapped onto the human genome (GRCh37 with annotation of GENCODE v27 lift37, <https://www.gencodegenes.org/>) using STAR (v2.5.3a, <https://cutadapt.readthedocs.io/en/stable/>). The gene expression (fragments per kilobase million, FPKM) was estimated by RSEM (v1.3.1, <https://deweylab.github.io/RSEM/>), and the relative fold changes were calculated. The hierarchical clustering of log<sub>2</sub> fold changes was performed using Cluster 3.0 (v10.0, <https://www.encodeproject.org/software/cluster/>) with centered correlation and average linkage parameter, the heatmap was visualized using TreeView (v2.0.8, [https://download.cnet.com/TreeView/3000-2352\\_4-75666005.html](https://download.cnet.com/TreeView/3000-2352_4-75666005.html)).

The Ribo-seq data were analyzed according to the method described by Calviello et al. [34]. The translation efficiency of each gene was estimated by dividing the transcripts per kilobase million (TPM) of ribosome-protected mRNAs by the relative transcript abundance. For the coverage plot, we scaled each transcript and divided 5'-UTR, CDS, and 3'-UTR regions to 20, 100, and 50 windows, respectively. The average coverage in each window was normalized to the mean coverage of the entire transcript. To assess the statistical changes in the translation efficiency, Ribo-seq signals and RNA-seq signals were analyzed using the Xtail pipeline [35], and the genes with adjusted P-values (less than 0.05) were used as differential translation efficiency genes.

## 3. Results

### 3.1. Identification of the interacting proteins of each PRMT

As protein modification enzymes, PRMTs dynamically interact with their protein substrates, complicating the identification of interacting partners. To systematically characterize the interactome of different PRMTs *in vivo*, we labeled interacting proteins with biotin using a highly sensitive BiolD technology. Based on previous reports that the N-terminus of PRMT is responsible for substrate recognition [19,36–38], we fused a promiscuous biotin ligase BirA\* (BirA<sup>R118G</sup>) to the C-terminus of each PRMT and expressed the fusion proteins in HEK293T cells. Using cell fractionation followed by Western blotting, we first confirmed that fusion proteins had a similar pattern of cytoplasmic versus nuclear localization and similar expression compared to endogenous PRMTs (Fig. S1 online, except for the PRMT8 that was poorly expressed in 293 T cells). After transient expression of each fusion protein for 48 h, we purified the total biotinylated proteins with streptavidin beads using stringent washing conditions (2% SDS). We subsequently conducted a label-free quantitative (LFQ) mass spectrometry using the MaxLFQ pipeline to quantify protein abun-



dance [25] (Fig. 1b, see Materials and methods and Supplementary materials online for details). We transfected all PRMT-BirA\* fusion proteins and mock control (BirA\* only) in three biological replicates. Only proteins with valid LFQ intensity values were considered; their average intensity was subsequently calculated. We identified putative interactors of each PRMT by evaluating protein quantification values, and scored the positive hits using an LFQ intensity cutoff of two-fold higher than that of the mock control (see Supplementary materials and Table S1 online).

Using Western blotting, we first confirmed that the proteins purified from cells transfected with PRMT-BirA\* were heavily biotinylated as compared with those from cells transfected with the BirA\* control (Fig. 1c, left), with the PRMT themselves being the most heavily biotinylated proteins (Fig. 1c, right). The LFQ intensities of all detected proteins (as calculated by label-free quantification) are highly correlated between different replicates of the same PRMT (Fig. S2a online), indicating the reliability of this procedure.

In total, we identified 2372 candidate proteins bound by at least one of the nine PRMTs (Table S1 and Fig. S2b online). The identified proteins included several known partners required for PRMT activities, such as the MEP50 (WDR77), RIOK, and pICLN, which form an active methyltransferase complex with PRMT5 [39,40]. In addition, many of the identified PRMT interactors significantly overlapped with the proteins identified in the earlier proteomic studies using antibodies against methylarginine-containing oligopeptides [17,21] (Fig. 1d), indicating the sensitivity of the BioID technology in identifying their substrates that could transiently interact with the enzymes. These proteins contain several known PRMT substrates, including histones and hnRNPs (Table S1 online). Furthermore, several of the known and newly identified PRMT-interacting proteins were validated by co-immunoprecipitation (co-IP) experiments using Myc-tagged PRMTs, confirming the reliability of the BioID approach (Fig. S2c online). Further analysis of the amino acid composition showed that the newly identified PRMT interactors contained a higher fraction of arginine as compared to all human proteins, re-confirming the enrichment of PRMT substrates (Fig. S2d online).

In addition to the methylation substrates, the interactome of PRMTs may include proteins that regulate PRMT functions. These could be missed in immunoprecipitation with anti-methylarginine antibodies. Notably, only 4% of our newly identified PRMT-interacting proteins (85 out of 2372 proteins) were collected in the IntAct online PPI database (<https://www.ebi.ac.uk/intact/>) (Fig. S2e online), indicating that our results significantly expanded the interactome of each PRMT. Certain newly identified proteins were PRMT-interacting proteins but not *bona fide* substrates. Therefore, the observed functional consequences might not be a direct outcome of arginine methylation. Moreover, low overlaps with known interacting partners could be attributed to certain false-positive interactors identified in the BioID approach, as well as low sensitivity in the current IntAct PPI database.

### 3.2. Substrate preference of individual PRMTs

To further determine the substrate preference of different PRMTs, we compared the newly identified putative substrates for each PRMT. Our results indicated that several proteins were recog-

nized by multiple PRMTs, suggesting a major substrate redundancy for each PRMT (Fig. S2f online). For example, 90 proteins were recognized by all nine PRMTs, and 961 proteins were recognized by at least four out of nine PRMTs tested (Fig. S2g online). We further examined the overlaps of interacting proteins between each pair of PRMTs (Fig. 1e, red, overlap significance; blue, the numbers of overlapped proteins) and found that PRMTs could be clustered into two groups based on the similarity of their interactomes: one group containing PRMT2, PRMT6, PRMT7, and PRMT9, whereas another group containing PRMT1, PRMT3, PRMT4, PRMT5, and PRMT8.

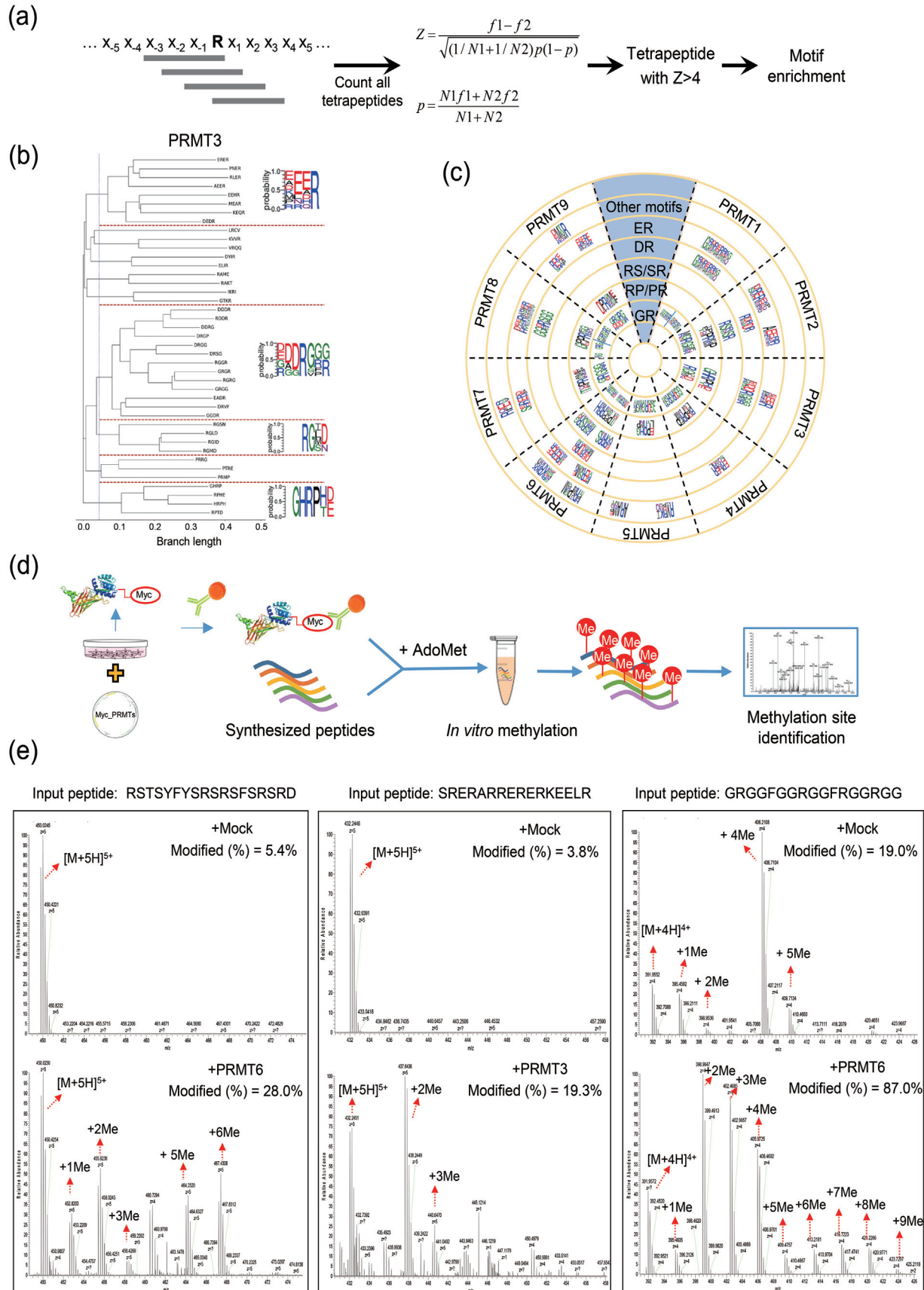
### 3.3. Identification and validation of consensus motifs for arginine methylation

Previous studies have reported that the glycine and arginine rich (GR-rich) motifs are preferably targeted for methylation by several PRMTs (including PRMT1, PRMT3, PRMT5, PRMT6, and PRMT8) [9,41,42]. However, additional consensus motifs, such as proline/glycine/methionine rich (PGM-rich) or RxR motifs, were found to be enriched near the methylarginine sites by mass spectrometry [43,44], suggesting that other sequences beside GR-rich motifs could be recognized as arginine methylation sites and that individual PRMTs had different preferences for their substrate.

To further determine the substrate preference for different enzymes, we analyzed the newly identified putative PRMT substrates by measuring the statistical enrichment of the sequences around the potential methylarginine (Fig. 2a, see Materials and methods for details). For each PRMT, the tetrapeptides around the potential methylarginine sites were compared with the arginine-containing tetrapeptides in all proteins obtained from the UniProt database to calculate the enrichment Z-scores (Fig. 2a). The enriched tetrapeptides were further clustered into different groups to obtain consensus motifs for arginine methylation by each PRMT. For example, the clusters and the consensus motifs for PRMT3 substrates are shown in Fig. 2b, and the clusters of all PRMTs are shown in Fig. S3 (online). We further compared the consensus motifs of all assessed PRMTs (Fig. 2c) and found that in addition to the known RGG motifs from the substrates of multiple PRMTs, several other new consensus motifs such as SR-rich, DR-rich, and ER-rich motifs were identified in PRMT substrates. These results provided a comprehensive profile for substrate preference of different PRMTs, suggesting that a diverse range of proteins could be potentially modified by PRMTs at different consensus motifs.

To validate the newly identified arginine methylation motifs, we selectively synthesized several peptides containing newly identified consensus motifs (SR-, ER-, and DR-rich motifs) and measured the methylation of arginine by cognate PRMTs using *in vitro* methylation reaction (Fig. 2d, Fig. S4c online). As a positive control, we used a peptide containing the GR-rich motif and measured its methylation by PRMT6. The peptides were incubated with purified PRMTs (Fig. S4a, b online) in the presence of methyl donor S-adenosylmethionine. The resulting samples were analyzed using mass spectrometry. We found that arginine residues within the newly identified motifs could be robustly methylated by cognate PRMTs, with the detection of both methylation and dimethylation, indicating that these newly identified consensus motifs were

**Fig. 1.** Systematic identification of PRMT interactome. (a) Schematic diagram showing PRMT1 to PRMT9. The light blue boxes represent the catalytic domains, the cyan and yellow boxes represent double E motifs and THW loop motifs that are specific to PRMTs, respectively. (b) Workflow for identifying PRMT-interacting proteins using BioID. (c) The biotinylated PRMT-interacting proteins detected by Western blotting using streptavidin-HRP (left) and silver staining (right). (d) The Venn diagram illustrating the PRMT interactome obtained from this study compared with methylarginine-containing proteins identified in the study by Larsen et al. (2016) and Guo et al. (2014). The correlation is calculated by Fisher's exact test, with the whole genome as the background. (e) Overlap of the interactome among different PRMTs. Fisher's exact test is used to calculate the *P*-value of the overlap. The PRMT interactomes are clustered by overlap significance (shown in red), and the numbers of overlapped protein are indicated in blue.



methylated at arginine residues. For example, SR-rich and DR-rich peptides could be methylated by PRMT2 and PRMT6 (Fig. 2e and Fig. S4d online). Furthermore, the DR-rich peptide could be methylated by PRMT1 at a considerably lower level compared with PRMT2 and PRMT6; however, it was poorly methylated by PRMT3 (data not shown). Interestingly, ER-rich peptides can only be methylated by PRMT3, whereas a relatively low level of methylations by other PRMTs was observed.

### 3.4. Potential functions of PRMT substrates

To examine the functional consequences of arginine methylation, we investigated the potential functions of newly identified PRMT substrates using GO analyses (<https://david.ncifcrf.gov/>) [45,46]. To increase the specificity of our analysis and reduce the statistical noises from numerous potential substrates, we first focused on proteins that were identified in both our dataset and in the dataset from earlier reports of methylarginine-containing proteins [17,21]. We found that these proteins were significantly enriched for biological processes involving RNA metabolisms, such as mRNA splicing, translation initiation, and mRNA export (Fig. 3a, left). Consistently, these proteins were enriched for RNA-binding domains such as RNA recognition motif (RRM), DEAD/DEAH RNA helicase, and KH domain (Fig. S5 online). The significant involvement of PRMT substrates in RNA metabolism supported the previous reports that many proteins with methylarginine modification participated in RNA processing [17,21]. In addition, other PRMT interactors that did not overlap with previously reported methylarginine-containing proteins were likely to be the regulator of PRMTs rather than their substrates (e.g., WDR77) or substrates that remained undetected in previous studies due to limitations of reagents/methodologies. Interestingly, these proteins were enriched in functions related to cell division/cell cycle and NF $\kappa$ B signaling (Fig. 3a, right). Moreover, these proteins were more enriched in domains involved in protein–protein interactions (e.g., Armadillo-type fold) and signal transduction (e.g., Ser/Thr protein kinase, TPR-like repeats) (Fig. S5 online).

Furthermore, we focused on candidates that formed dense protein–protein interaction (PPI) networks, as confirmed by the STRING database. We plotted the putative substrates regarding each PRMT (Fig. 3b) and found that the majority of these proteins were primarily involved in RNA processing and formation of the RNP complex. These proteins can be divided into two main groups: one containing the splicing regulatory factors and the other, including proteins in mRNA translation such as the ribosomal proteins (Fig. 3b). In addition, the core ribosomal proteins and the splicing factors identified in our study had a significantly higher frequency of arginine as compared with all human proteins (Fig. 3c), further supporting the extensive methylarginine modification observed in these proteins.

### 3.5. PRMT inhibitions alter alternative splicing of RNAs

The majority of human genes undergo alternative splicing (AS), which is generally regulated by various RNA-binding proteins (i.e.,

splicing factors) that recognize regulatory *cis*-elements to promote or suppress the use of adjacent splice sites [47]. It was previously reported that certain PRMTs (e.g., PRMT4, PRMT5, and PRMT6) affect splicing by modifying selected splicing factors or proteins involved in spliceosome maturation [43,48–52]. Because several proteins involved in regulating splicing were identified as PRMT substrates (Fig. 3b), we examined the impact of PRMT inhibition on AS. We successfully silenced six different PRMTs using shRNAs (Fig. S6a online) and studied their effect on splicing using RNA-seq (Fig. 4a). For each PRMT, we identified AS events that were significantly altered in PRMT knockdown cells as compared with the control cells transfected with scrambled shRNA (Fig. 4a).

RNAi of different PRMTs significantly changed the splicing in hundreds of genes harboring several AS types (Fig. 4b). Several AS events are affected by inhibiting more than one PRMT (i.e., large overlaps between splicing targets of different PRMTs), suggesting that arginine methylation of proteins by PRMTs regulates AS (Fig. 4c). Interestingly, the inhibition of different PRMTs exerted similar effects on the splicing of specific genes (i.e., the  $\Delta$ PSI were either positive or negative in most affected genes, Fig. 4d), implying that the methylation of the same RNA-binding proteins by different PRMTs produced similar effects on their activities. The splicing changes in selected AS events were further validated using semi-quantitative RT-PCR that reflected the splicing shift between different splicing isoforms following PRMT knockdown. For example, the splicing of a retained intron in the SEPT3 (neuronal-specific septin-3) gene was promoted by inhibition of all six PRMTs evaluated (Fig. 4e), and many other genes underwent AS in the same direction (Fig. S6b online), supporting the consistent regulation of splicing by different PRMTs.

### 3.6. Ribosomal proteins are extensively arginine methylated

Our gene ontology and protein–protein interaction analyses further revealed that proteins involved in mRNA translation were significantly enriched in the newly identified PRMT substrates, including greater than 50% core components of ribosomes (42 out of 80 ribosome proteins) and several canonical translation factors (EIF4G1, EIF4B, and EIF2A). Table S2 (online) lists 80 human core ribosome proteins with newly identified interacting PRMTs and putative methylarginine sites. Our finding was consistent with that of earlier reports in the late 1970s that both subunits of the ribosome contained methyl arginine as confirmed by chromatography of ribosomal proteins-originated short peptides or amino acid residues [53–55]. Furthermore, several ribosomal proteins were recently reported to contain methylarginine, including yeast RPL12 and RPS2 [56] and human RPS3 and RPS10 [57,58]. The extensive arginine methylation observed in core ribosomal proteins suggested a critical function of this kind of PTM in protein translation.

To directly test this hypothesis, we performed polysome profiling to isolate different ribosome fractions (40S, 60S, 80S, and polysome, Fig. 5a) and evaluated their methylation status using anti-pantarginine methylation antibodies (Fig. 5b). Our data demonstrated that ribosomal proteins (most having a molecular weight

**Fig. 2.** Identification and validation of consensus motifs for arginine methylation. (a) Schematic diagram for identification of enriched motifs in the PRMT interactome. All tetrapeptides around arginine were counted, and the frequencies of each tetrapeptide in PRMT interactomes were compared with the background of all human proteins to identify enriched tetrapeptides (see Materials and methods). (b) The clustering of enriched tetrapeptides in the PRMT3 interactome is shown as an example. The enriched tetrapeptides were collected as input in Clustalw2 (v2.0.9) to generate hierarchical dendograms. The consensus motifs were listed beside each group. (c) A summary of all enriched motifs found in each PRMT interactome. Similar motifs are placed in the same concentric circle. (d) The experimental workflow of *in vitro* methylation and identification of methylarginine-containing peptides. R<sup>Me</sup> and R<sup>2Me</sup> are set as dynamic modifications with a mass shift of 14.01565 and 28.0313, respectively. (e) The arginine methylation pattern of representative peptides from newly identified R-methylation motifs (SR-rich and ER-rich motifs) and the known GR-rich motif was measured by mass spectrometry. In each case, the upper spectrum indicates the negative control without adding enzymes, and the lower spectrum shows the methylarginine signals after *in vitro* methylation. For each peptide, the ratio of methylation was calculated as the sum of the peak areas from the TIC values of the modified peptides divided by the peak area of total peptides.

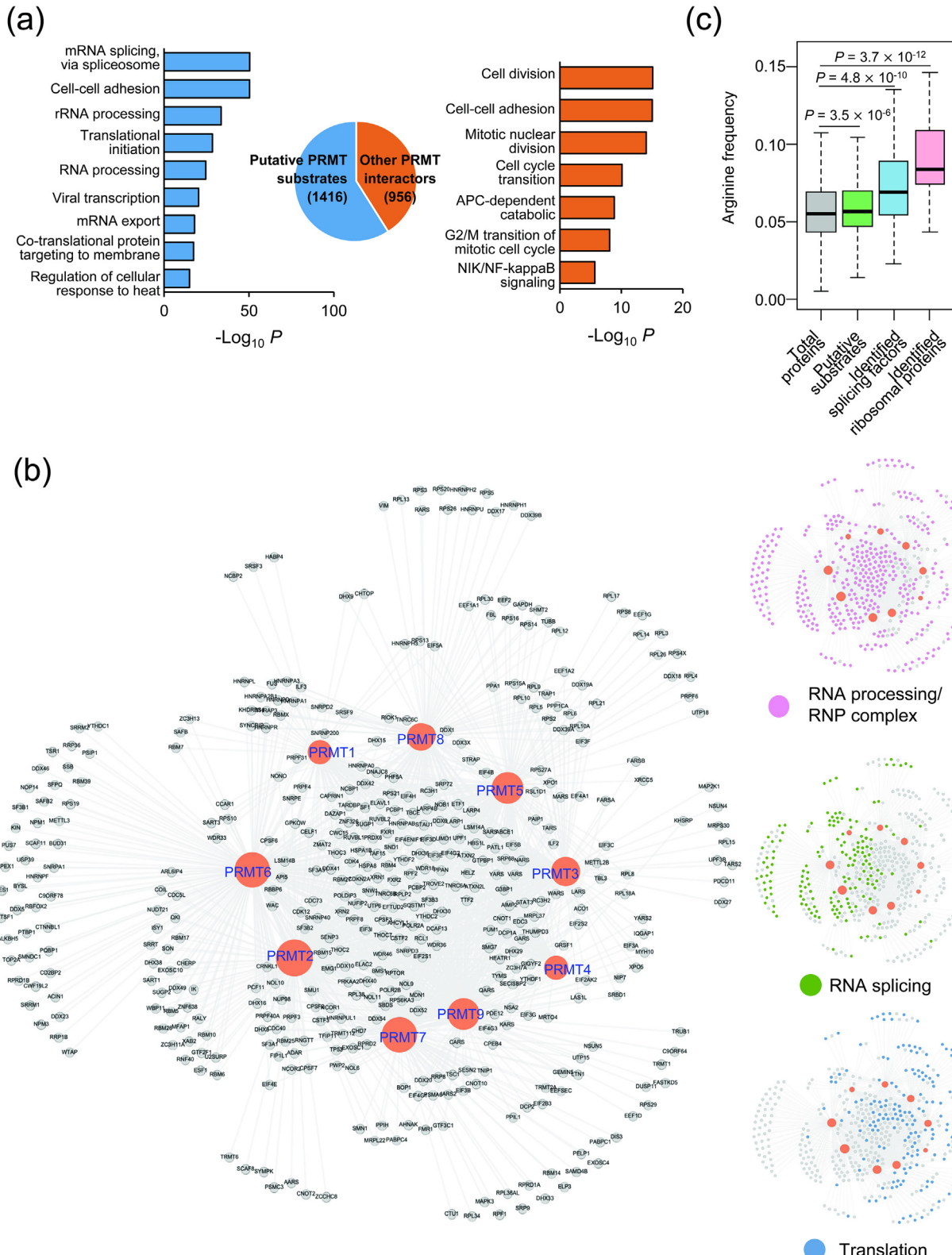


**Fig. 3.** Arginine methylation is highly involved in RNA splicing and translation. (a) Gene ontology analysis of 1416 putative PRMT substrates detected in both the present study and previously identified methylarginine-containing proteins (putative PRMT substrates, blue bars), as well as other PRMT-interacting proteins identified only in the present study (orange bar). X-axis: BH-adjusted  $P$ -values ( $-\log_{10}$  scale). (b) Connectivity map of nine PRMTs (brown circles) and their putative substrates (left). Moreover, putative substrates were classified and colored according to their major functions (right). (c) Arginine frequency of all annotated human proteins ( $n = 42,119$ ), identified putative PRMT substrates ( $n = 1416$ ), identified splicing factors with methylarginine ( $n = 148$ ), and identified ribosomal proteins as PRMT substrates ( $n = 42$ ). Wilcoxon test was used to calculate the  $P$ -value.

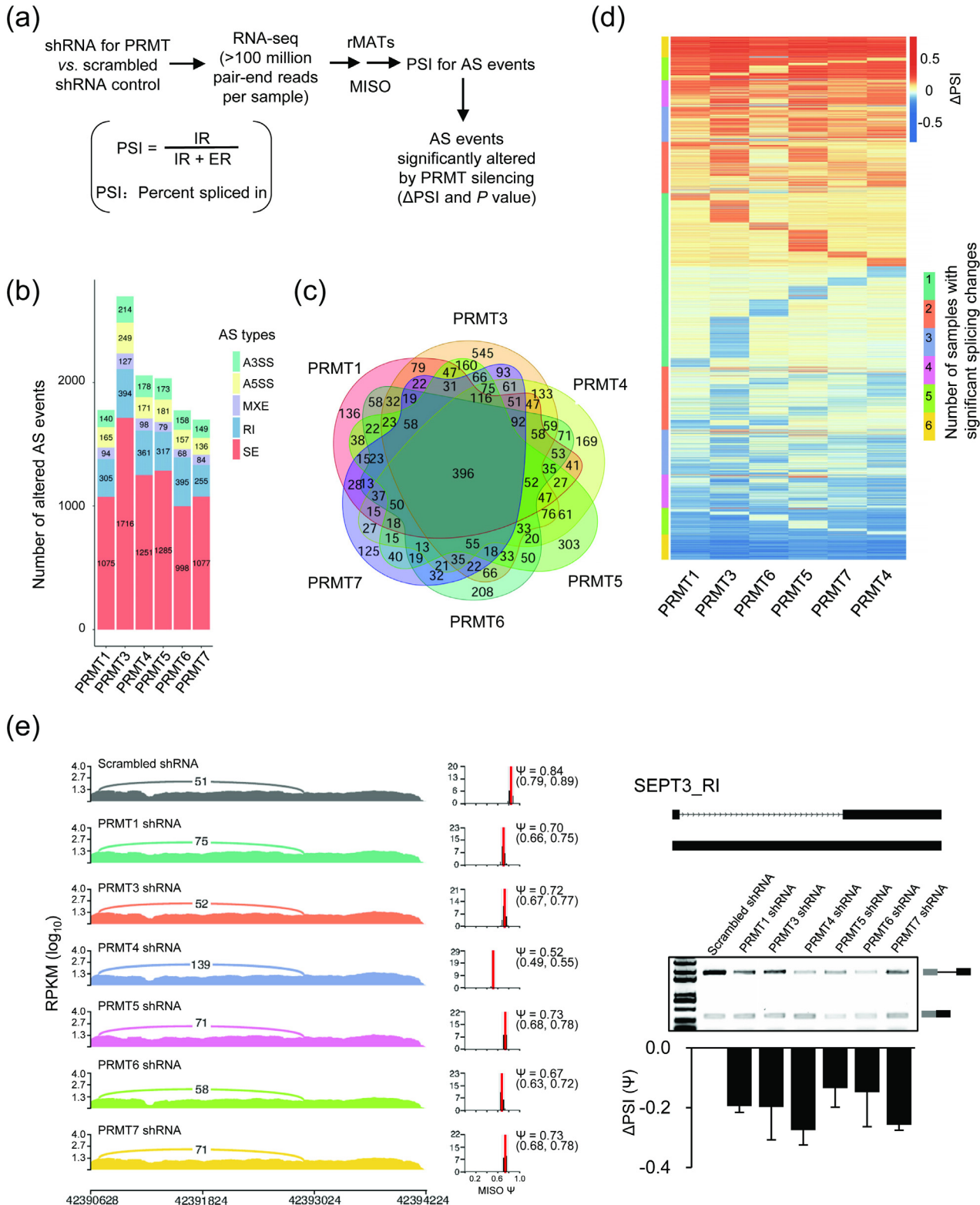


**Fig. 4.** PRMT inhibition globally alters alternative splicing. (a) Workflow showing RNA splicing for PRMT knockdown samples using RNA-seq and analyzed by the rMATs pipeline to calculate the PSI values. We used  $|\Delta\text{PSI}| > 0.1$  and read counts greater than 50 as the cutoff to identify significantly altered splicing events. (b) Count of different kinds of AS events after PRMT knockdown. A3SS, alternative 3' splice site; A5SS, alternative 5' splice site; MXE, mutually exclusive exon; RI, retained intron; SE, skipped exon. (c) The intersection of altered AS events following the silencing of different PRMTs. (d) All AS events altered following the silencing of each PRMT were colored according to  $\Delta\text{PSI}$ . Moreover, the AS events were clustered by the numbers of PRMT RNAi samples with significant splicing changes (e.g., the clusters labeled in yellow include AS events affected by RNAi of all six PRMTs assessed). (e) Experimental validation of splicing alteration. Sashimi plot of splicing change in SEPT3 is presented on the left, including the counts of junction read, the PSI value, and its confidence interval. Representative semi-quantitative PCR is shown on the right (three biological replicates were performed). Additional examples of altered AS events can be found in Fig. S6b (online).

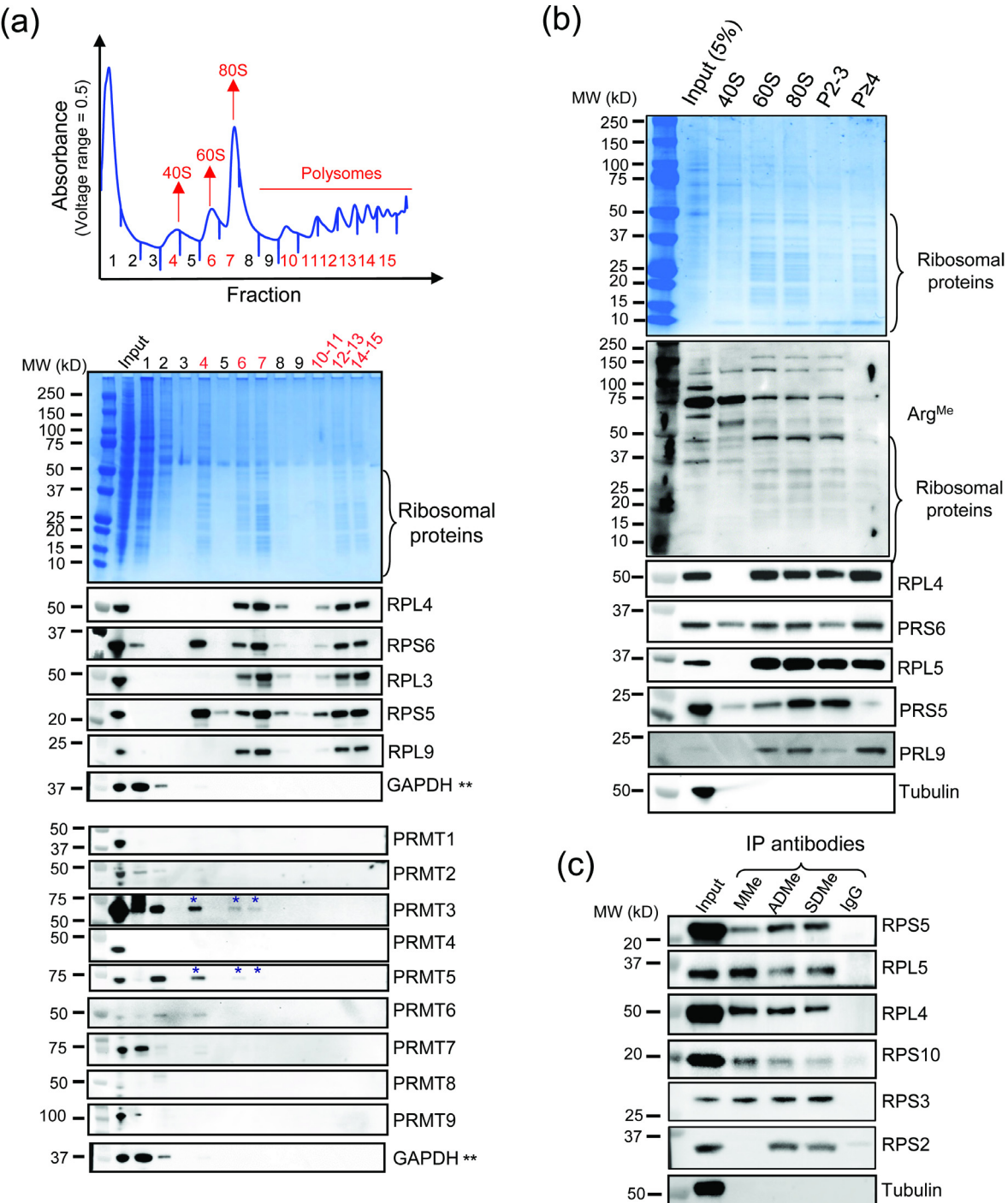
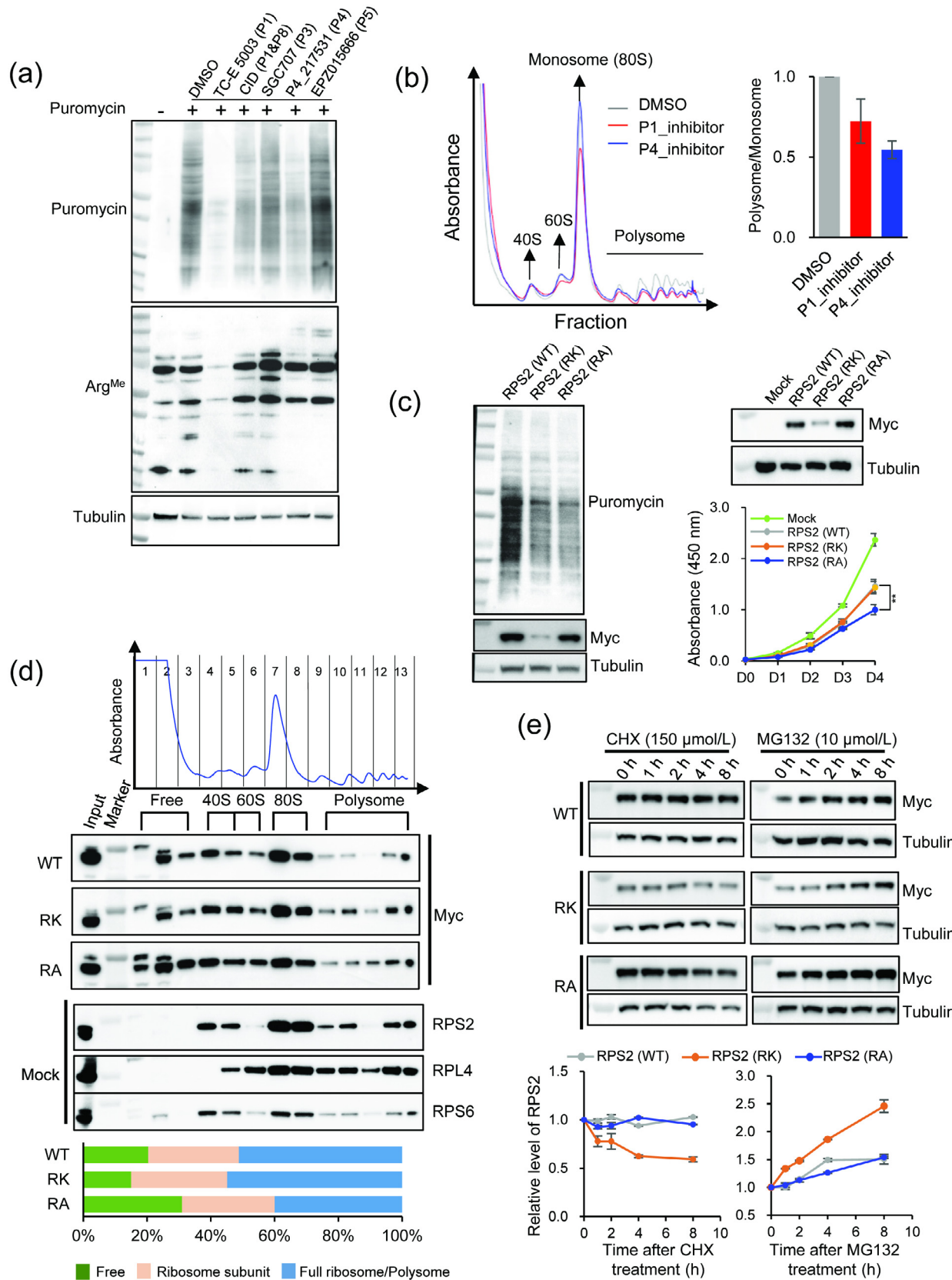


**Fig. 5.** Ribosomal proteins are extensively methylated. (a) Fractionation of polysomes using HEK293T cell lysis. Each fraction was collected, and proteins in each fraction were precipitated for SDS-PAGE. Both Coomassie blue staining (top) and Western blotting (bottom) were used to detect proteins in each fraction. Accumulation of ribosomal proteins can be observed on the gel (MW between 15 and 50 kD, middle). (b) The arginine methylation of ribosomal proteins was detected by a combination of anti-pan-methylarginine antibodies that recognized MMA, aDMA, and sDMA. (c) The HEK293T cell lysate was immunoprecipitated with different anti-methylarginine antibodies, and the selected ribosomal proteins were detected with Western blotting.\* indicates that a small fraction of PRMT3 and PRMT5 co-separated with both ribosomal subunits.\*\* indicates that the two figures were the same.

(MW) ranging from 10 to 50 kD) were extensively R-methylated in different ribosome profiling fractions (Fig. 5b). Moreover, several ribosomal proteins were detected in the precipitates pulled down by different anti-methylarginine antibodies (anti-MMA, aDMA, and sDMA antibodies) (Fig. 5c), concluding that ribosome proteins were extensively methylated at arginine residues. Our observation that most PRMTs were not co-purified with ribosomes (Fig. 5A)

was consistent with the absence of PRMTs from the known *ribo*-interactome [59]. Interestingly, a small fraction of PRMT3 and PRMT5 co-separated with both ribosomal subunits (the 40S and to a lesser extent the 60S) but not with the assembled 80S ribosome and polysomes (Fig. 5a, indicated by asterisks). This finding is consistent with previous reports that PRMT3 formed an active enzyme complex with RPS2 to catalyze RPS2 methylation [60–62].



### 3.7. Arginine methylation is critical for the assembly and function of ribosomes

Based on the extensive arginine methylation of ribosomal proteins and translation factors, we hypothesized that PRMT inhibition could affect the global translation. To test this hypothesis, we used puromycin incorporation assay to study global protein synthesis in three different cell lines following treatment with PRMT-specific inhibitors (Fig. 6a and Fig. S7a online). We used chemical inhibitors of PRMTs because they could provide a more rapid suppression of ribosomal activity that might otherwise be compensated in cells with stable knockdown of PRMTs.

We found that the inhibitors of PRMT1 and PRMT4/CARM1 effectively reduced arginine methylation and global protein synthesis across different cell lines (Fig. 6a and Fig. S7a online). Furthermore, the inhibition of these two PRMTs produced the most obvious reduction in arginine methylation. Polysome profiling revealed that the inhibition of PRMT1 or PRMT4 effectively reduced the abundance of polysomes versus monosomes (Fig. 6b and Fig. S7a online), suggesting a global reduction of mRNAs undergoing active translation. As expected, we found that PRMT1 or PRMT4 inhibitors dramatically delayed cell growth, consistent with the general inhibition of protein translation (Fig. S7b, c online). Moreover, shRNA-mediated knockdown of PRMT1 and PRMT4 reduced the translation efficiency as confirmed by polysome occupancy (Fig. S7d online); however, we used inhibitors for further experiments because these allowed examining how the methylation deficiency affected RNA translation before the cells developed a compensation effect from RNAi.

To further examine the potential mechanisms of how arginine methylation affected mRNA translation, we selected the ribosomal protein RPS2, a newly identified PRMT1 and PRMT4 substrates in our dataset. RPS2 has an N-terminal GR-rich motif, which is a consensus motif for efficient arginine methylation. We introduced two mutations into the potential methylarginine sites (6RA and 6RK, with six Arg substituted by Ala or Lys, respectively, Table S2 online) to examine if such mutations affected the assembly of RPS2 into the ribosomes. We expressed the wild type and mutated RPS2 in HEK293 cells and found that the translation was inhibited by RPS2 mutations (Fig. 6c, left panel). In addition, the cell proliferation was slightly delayed following transient expression of RPS2–6RA (Fig. 6c, right), probably because of disruption of ribosomal assembly/function due to an altered riboprotein ratio [63].

We further used polysome profiling to determine the efficiency of different RPS2s in assembling into a ribosomal complex. Although the endogenous RPS2 was mostly assembled into either ribosomal subunit or complete ribosome/polysome in control cells, a notable fraction of transiently expressed RPS2s was present in the fraction of free proteins (Fig. 6d and Fig. S8 online). We found that compared with the wild type, the RPS2-RA mutation with defective methylation sites resulted in an assembly defect, with

more proteins found in the free fraction. Interestingly, the RPS2-RK mutation exhibited an opposite effect, with fewer proteins in the free fraction and more in the complete ribosome/polysome (Fig. 6d). Because lysine residues can undergo several PTMs, including methylation and ubiquitination, we speculated that the phenotype of RPS2-RK mutation could be affected by other factors. The RPS-RK mutation was expressed at a lower level as compared with wild type RPS2 or RA mutation (Fig. 6c). Inhibiting translation with cycloheximide (CHX) revealed that RPS-RK was degraded more rapidly than the wild type RPS2 and RA mutation that were considerably stable (Fig. 6e). Moreover, inhibition with MG132 significantly increased the level of RPS2-RK as compared with WT and RA mutation, suggesting that RPS2-RK was degraded through a ubiquitin-dependent pathway (Fig. 6e).

### 3.8. PRMT activity inhibition causes global translation deficiency

To further examine how PRMT inhibitions affected the translation of different mRNAs, we sequenced the mRNA population present in different ribosomal fractions following treatment with PRMT1 and PRMT4 inhibitors (Fig. 7a). Compared with the control samples treated with DMSO, the inhibition of PRMTs significantly reduced the level of mRNAs bound by single ribosomes or polysomes (Fig. 7b). More specifically, among the 6783 protein-coding genes detected with reliable numbers of RNA-seq reads, 4392 mRNAs in the PRMT1-inhibited sample (~65%) and 3830 mRNAs in the PRMT4-inhibited sample (~56%) showed a consistent decrease in the association with different ribosomal fractions (i.e., both monosomes and polysomes), suggesting a reduced translation on most mRNAs (Fig. 7c). Interestingly, the GO analysis of these mRNAs did not produce any functional enrichment (data not shown), confirming a global reduction in mRNA translation rather than translation inhibition on a specific subgroup of mRNAs.

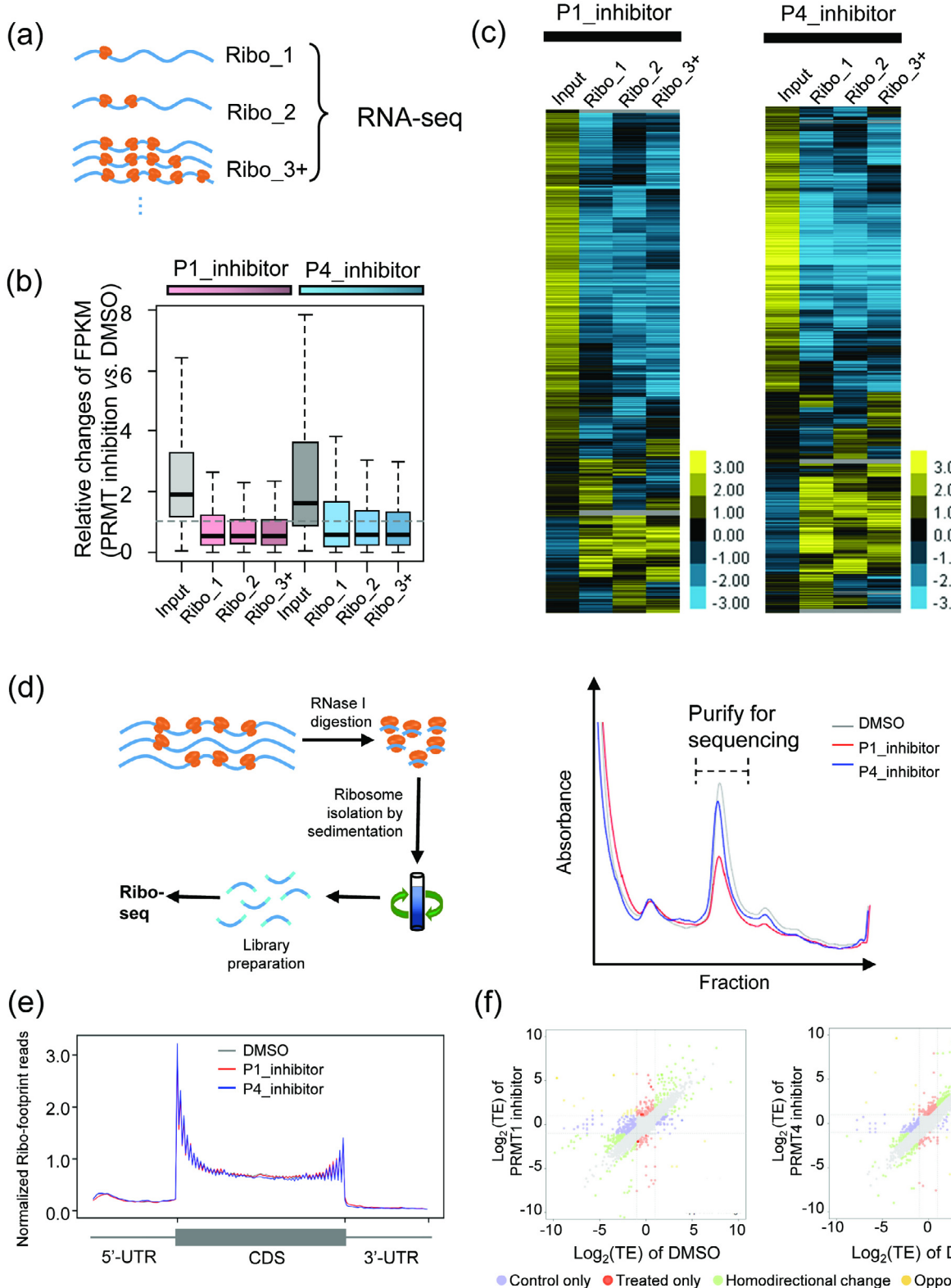
We next determined how PRMT inhibition affected the translation of different mRNAs using Ribo-seq and measured the distribution of ribosome-protected RNA fragments in control and PRMT inhibition samples (Fig. 7d). This analysis generated a “snapshot” of all mRNAs that are occupied by active ribosomes (i.e., undergoing active translation) in a cell at a particular condition [64]. As expected, the ribosome occupancy is higher in the coding region compared to the 5' and 3' UTRs following normalization against average coverage (Fig. 7e). In addition, the binding of ribosomes to mRNAs was slightly enriched in the region around the start codon and before the stop codon, suggesting a ribosome pausing after the initiation and delayed ribosome release (Fig. 7e). This is consistent with the ribosomal profiling results obtained from other groups [64]. Interestingly, we found that the inhibition of PRMT activity did not change the distribution of ribosome occupancy in different regions of mRNAs (Fig. 7e). Given the translation reduction by PRMT inhibitors (Fig. 6a, b and Fig. 7b, c), this result suggested that PRMTs affected the maturation of ribosomes before they are assembled onto the mRNAs, consistent with our finding

**Fig. 6.** Arginine methylation affects translation efficiency and assembly of ribosomal proteins. (a) Puromycin incorporation assay to study translation efficiency following inhibition of specific PRMTs. HEK293T cells were treated with different PRMT inhibitors for 24 h, and puromycin was added 30 min before cell harvest. The incorporation of puromycin was detected by Western blotting using the anti-puromycin antibody. The anti-pan-methylarginine antibody was used to measure changes in the arginine methylation status. (b) The effect of PRMT inhibition on ribosome fractions. HEK293T cells treated with PRMT1 (TCE-5003) and PRMT4 (217531) inhibitors were analyzed using polysome profiling, and the percentage of monosomes versus polysomes was calculated using the peak areas. In the two biological replicates, the percentage in each drug-treated sample was normalized to that in the DMSO control. (c) Myc-tagged wild-type or mutated RPS2 was expressed in HEK293T cells, and the translation efficiency was examined using puromycin incorporation assay. The cell proliferation was studied for 4 d after 24 h transfection, and two biological replicates were performed. \*\*Indicates that the *P*-value is less than 0.01 using Student's *t*-test. (d) Arginine methylation of RPS2 affects ribosome assembly. Myc-RPS2(WT), Myc-RPS2(6RK), and Myc-RPS2(6RA) were transfected into HEK293T cells for 48 h, followed by polysome profiling. Fractions were collected, and the assembly of RPS2 was detected using Western blotting with an anti-Myc antibody. The mock control fractions were also detected with an anti-RPS2 antibody. Anti-RPS6 and anti-RPL4 antibodies were used as ribosomal profiling markers. (e) Protein degradation of wild type and mutated RPS2 following transfection and treatment by cycloheximide (CHX) or MG132 was measured. The HEK293T cells were transfected with an equal amount of Myc-RPS2(WT), Myc-RPS2(6RK), and Myc-RPS2(6RA), and the drugs were added 36 h following transfection. The protein levels were detected by Western blotting at different time points (h) following drug treatment. Three biological replicates were performed. \*\* indicates that the *P*-value is less than 0.01 using Student's *t*-test.

that arginine methylation of ribosomal proteins was essential for ribosome assembly.

We further determined specific genes whose translation efficiency (TE) was preferably affected by PRMT inhibition using the

Xtail pipeline [35] to measure the genes with significant TE changes following PRMT inhibition (Fig. 7f). We found that PRMT1 inhibition significantly changed the TE of only eight coding genes, whereas the TE of 46 protein-coding genes was significantly



altered following PRMT4 inhibition (Fig. 7f). Interestingly, among the 46 genes affected by PRMT4 inhibition, 25 ribosomal protein genes had significantly increased TE, suggesting a potential functional compensation following translation suppression.

#### 4. Discussion and conclusion

Although a common PTM, arginine methylation is a relatively understudied modification. Numerous proteins undergo methylation at their arginine residues [5,7,65]. Several PRMTs catalyze this kind of PTM; however, the relationship between PRMTs and their substrates has not been established on a global scale. We identified the putative substrates for each of the human PRMTs and further characterized the novel consensus methylation motifs for individual human PRMTs. We found a high degree of overlap in the substrate specificity of different PRMTs, as well as significant enrichment for RNA-binding proteins in the substrates of all PRMTs. In particular, the splicing factors and ribosomal proteins are heavily methylated and overrepresented as PRMT substrates. Furthermore, PRMT inhibition causes a global deficiency of RNA translation. Collectively, the identification and characterization of substrates for all human PRMTs provide a basis for further studies on their biological functions.

The majority of the consensus motifs for arginine methylation are short fragments with low sequence complexity, including the well-known GR-rich motifs and newly identified SR- and ER-rich motifs (Fig. 2 and Fig. S3 online). Because low-complexity domains (e.g., GR- and SR-rich domains in RNA-binding proteins) usually form a non-structural region, the recognition by PRMTs likely occurs in the unstructured regions of proteins. This observation suggests a structure-independent recognition that supports promiscuous binding between PRMTs and their targets. This binding could explain the high overlaps between the binding partners of different PRMTs, suggesting a certain degree of functional redundancy among PRMTs. Moreover, the knockout mice of most PRMTs have only mild phenotypes [14,66,67], except for PRMT1 and PRMT5 that caused lethal phenotypes following knockout [68–70], and PRMT4 whose knockout can cause death after birth in mice [71]. Therefore, we speculated that the additional specificity was provided by the spatial/temporal control of expression of PRMTs and their potential targets.

Because arginine methylation increases protein hydrophobicity, it could affect how proteins interact with their partners and assemble into a functional complex. We found core ribosomal proteins as the largest protein groups recognized and methylated by PRMTs, increasing the possibility that the methylarginine modification of ribosomal proteins affected the assembly and function of ribosomes. It is well known that ribosome heterogeneity regulates mRNA translation [72,73]; therefore, we speculated the methylarginine modification status of ribosomal proteins as a major source of ribosome heterogeneity. We demonstrated that mutations in the methylation sites of RPS2 inhibited its assembly onto ribosomes and found that inhibitions of certain PRMTs globally

suppressed translation. Rather than affecting a specific step of translation, our data implied that the translation could be reduced due to defects in ribosome biogenesis before ribosomes are assembled onto mRNAs.

Although the ribosomal proteins are significantly enriched with arginine residues and are the most overrepresented targets of PRMTs, we speculated that they are differentially modified by different PRMTs. Consequently, inhibition of different PRMTs affected the translation efficiency of distinct sets of mRNAs. More detailed analyses on how each PRMT differentially affects the assembly and functions of ribosomes will be an important subject for future studies.

Like other PTMs, methylation of arginine could have specific “readers”, “erasers”, and “writers”. Although nine PRMTs were identified as methylarginine writers, only one “eraser protein,” JMJD6, has been reported for methylarginine [74]. Moreover, several proteins containing “Tudor” domains were proposed to function as putative “readers” [75–77]. We expect that the biological functions of methylarginine modification are probably determined by networks consisting of different “writers,” “erasers”, “readers”, and their substrates. Therefore, mapping such interacting networks will provide useful information on the functions of arginine methylation in several proteins. This study represents a start point for the comprehensive mapping of a network containing methylarginine “writers,” “erasers,” “readers” and their substrates, thus serving as a reference for future research.

#### Declaration of competing interest

The authors declare that they have no conflict of interest.

#### Acknowledgments

We thank Han Yan at Omics Core of Bio-Med Big Data Center, CAS-MPG Partner Institute for Computational Biology (PICB), for assistance with next-generation sequencing. Yu-Jie Chen at Uli Schwarz Quantitative Biology Core Facility, PICB, for experimental support with this study, and Prof. YanZhong Yang and Prof. Mark T. Bedford at the University of Texas MD Anderson Cancer Center for their generous gift of several PRMT plasmids. This work was supported by the National Natural Science Foundation of China (31730110, 31661143031, 91940303, and 91753135), the Science and Technology Commission of Shanghai Municipality grant (17JC1404900, 18XD1404400, and 20ZR1467300), and a Joint Research grant with State Key Laboratory of Microbial Metabolism, School of Life Science and Biotechnology, Shanghai Jiao Tong University (MMLKF16-11).

#### Author contributions

Huan-Huan Wei and Zefeng Wang conceived the project. Huan-Huan Wei, Meng Guo, and Miao-Wei Mao carried out the molecular and biochemical experiments. Xiao-Juan Fan, Yue Hu, and Zhao-

**Fig. 7.** Inhibition of PRMT activity causes global translation deficiency in thousands of genes. (a) Schematic representation of experiments. Polysome profiling was performed to fractionate different ribosome fractions following treatment with PRMT inhibitors in HEK293T cells. The mRNAs bound to one ribosome (ribo\_1), two ribosomes (ribo\_2), and more than three ribosomes (ribo\_3+) were collected and subjected to RNA-seq, respectively. (b) The relative FPKM changes in the input mRNAs and ribosome-bound mRNAs (with PRMT1 and PRMT4 inhibition compared with DMSO control) were represented as box plots. (c) Hierarchical clustering of different mRNAs in the input and ribosome-bound fractions following treatment with PRMT1 and PRMT4 inhibitors. The log<sub>2</sub> fold change in each mRNA was calculated and hierarchically clustered. (d) The samples with PRMT1 and PRMT4 inhibition were treated with RNase I to collect ribosome-protected RNAs for high-throughput sequencing (Ribo-seq assay). The schematic representation of experiments (left panel) and the isolated ribosome fractions for sequencing (right panel) are shown. (e) Ribosome-protected RNA reads were mapped to the human genome, with the number of ribosome footprint reads in the different regions of transcripts normalized by average coverage of each transcript. All transcripts were combined to plot the distribution of normalized reads along the transcript regions. (f) Changes in translation efficiency (TE) following PRMT inhibition. Changes in each transcript were plotted as a scatter plot (more significant P-values presented with a darker color). Blue: genes with large TE changes only in the control sample; red: genes with homodirectional changes in TE under two conditions; green: genes with opposite changes in TE under two conditions.

Yuan Fang analyzed the RNA-seq and Ribo-seq data as well as did other bioinformatic analyses. Xiao-Xu Tian, Ping Wu, Shuai-Xin Gao, and Chao Peng conducted mass spectrometry experiments. Xiao-Juan Fan, Yue Hu, Yun Yang, Xiao-Xu Tian, Huan-Huan Wei, and Zefeng Wang were responsible for study design and interpretation of data. All authors were involved in drafting the manuscript and revising it critically for important intellectual content.

## Appendix A. Supplementary materials

Supplementary materials to this article can be found online at <https://doi.org/10.1016/j.scib.2021.01.004>.

## References

- [1] Paik WK, Kim S. Omega-n-methylarginine in protein. *J Biol Chem* 1970;245:88–92.
- [2] Baldwin GS, Carnegie PR. Specific enzymic methylation of an arginine in the experimental allergic encephalomyelitis protein from human myelin. *Science* 1971;171:579–81.
- [3] Kakimoto Y. Methylation of arginine and lysine residues of cerebral proteins. *Biochim Biophys Acta* 1971;243:31–7.
- [4] Gary JD, Clarke S. RNA and protein interactions modulated by protein arginine methylation. *Prog Nucleic Acid Res* 1998;61:65–131.
- [5] Ong S-E, Mittler G, Mann M. Identifying and quantifying *in vivo* methylation sites by heavy methyl silac. *Nat Methods* 2004;1:119–26.
- [6] Bedford MT, Richard S. Arginine methylation: an emerging regulator of protein function. *Mol Cell* 2005;18:263–72.
- [7] Pahllich S, Zakaryan RP, Gehring H. Protein arginine methylation: Cellular functions and methods of analysis. *Biochim Biophys Acta* 2006;1764:1890–903.
- [8] Bedford MT. Arginine methylation at a glance. *J Cell Sci* 2007;120:4243–6.
- [9] Blanc RS, Richard S. Arginine methylation: The coming of age. *Mol Cell* 2017;65:8–24.
- [10] Sylvesteren KB, Horn H, Jungmichel S, et al. Proteomic analysis of arginine methylation sites in human cells reveals dynamic regulation during transcriptional arrest. *Mol Cell Proteomics* 2014;13:2072–88.
- [11] Peng C, Wong CCL. The story of protein arginine methylation: Characterization, regulation, and function. *Expert Rev Proteomics* 2017;14:157–70.
- [12] Chong PA, Vernon RM, Forman-Kay JD. Rgg/rg motif regions in rna binding and phase separation. *J Mol Biol* 2018;430:4650–65.
- [13] Lorton BM, Shechter D. Cellular consequences of arginine methylation. *Cell Mol Life Sci* 2019;76:2933–56.
- [14] Yang Y, Bedford MT. Protein arginine methyltransferases and cancer. *Nat Rev Cancer* 2013;13:37–50.
- [15] Poulard C, Corbo L, Le Romancer M. Protein arginine methylation/demethylation and cancer. *Oncotarget* 2016;7:67532–50.
- [16] Stuhlinger MC, Tsao PS, Her J-H, et al. Homocysteine impairs the nitric oxide synthase pathway: Role of asymmetric dimethylarginine. *Circulation* 2001;104(21):2569–75.
- [17] Larsen SC, Sylvesteren KB, Mund A, et al. Proteome-wide analysis of arginine monomethylation reveals widespread occurrence in human cells. *Sci Signal* 2016;9:rs9.
- [18] Radzishevskaya A, Shliaha PV, Grinev V, et al. Prmt5 methylome profiling uncovers a direct link to splicing regulation in acute myeloid leukemia. *Nat Struct Mol Biol* 2019;26:999–1012.
- [19] Shishkova E, Zeng H, Liu F, et al. Global mapping of carm1 substrates defines enzyme specificity and substrate recognition. *Nat Commun* 2017;8:15571.
- [20] Musiani D, Bok J, Massignani E, et al. Proteomics profiling of arginine methylation defines prmt5 substrate specificity. *Sci Signal* 2019;12:eaat8388.
- [21] Guo A, Gu H, Zhou J, et al. Immunoaffinity enrichment and mass spectrometry analysis of protein methylation. *Mol Cell Proteomics* 2014;13:372–87.
- [22] Roux KJ, Kim DL, Burke B, et al. BioID: a screen for protein-protein interactions. *Curr Protoc Protein Sci* 2018;91:19.23.1–19.23.15.
- [23] Roux KJ, Kim DL, BioID B. BioID: A screen for protein-protein interactions. *Curr Protoc Protein Sci* 2013;74:19.23.1–19.23.14.
- [24] Roux KJ, Kim DL, Raida M, et al. A promiscuous biotin ligase fusion protein identifies proximal and interacting proteins in mammalian cells. *J Cell Biol* 2012; 196: 801–10.
- [25] Cox J, Hein MY, Luber CA, et al. Accurate proteome-wide label-free quantification by delayed normalization and maximal peptide ratio extraction, termed maxLFQ. *Mol Cell Proteomics* 2014;13:2513–26.
- [26] Fairbrother WG, Yeh RF, Sharp PA, et al. Predictive identification of exonic splicing enhancers in human genes. *Science* 2002;297:1007–13.
- [27] Cheng D, Vemulapalli V, Bedford MT. Methods applied to the study of protein arginine methylation. *Methods Enzymol* 2012;512:71–92.
- [28] Lin C-J, Robert F, Sukarieh R, et al. The antidepressant sertraline inhibits translation initiation by curtailing mammalian target of rapamycin signaling. *Cancer Res* 2010;70:3199–208.
- [29] Vyas K, Chaudhuri S, Leaman DW, et al. Genome-wide polysome profiling reveals an inflammation-responsive posttranscriptional operon in gamma interferon-activated monocytes. *Mol Cell Biol* 2009;29:458–70.
- [30] Kelleher AR, Kimball SR, Dennis MD, et al. The mtorc1 signaling repressors reddl1/2 are rapidly induced and activation of p70s6k1 by leucine is defective in skeletal muscle of an immobilized rat hindlimb. *Am J Physiol Endocrinol Metab* 2013;304:E229–36.
- [31] Ingolia NT, Brar GA, Rouskin S, et al. The ribosome profiling strategy for monitoring translation *in vivo* by deep sequencing of ribosome-protected mRNA fragments. *Nat Protoc* 2012;7:1534–50.
- [32] Szklarczyk D, Franceschini A, Wyder S, et al. String v10: Protein-protein interaction networks, integrated over the tree of life. *Nucleic Acids Res* 2015; 43: D447–52..
- [33] Hu Y. Efficient, high-quality force-directed graph drawing. *Mathematica J* 2005;10:37–71.
- [34] Calviello L, Mukherjee N, Wyler E, et al. Detecting actively translated open reading frames in ribosome profiling data. *Nat Methods* 2016;13:165–70.
- [35] Xiao Z, Zou Q, Liu Y, et al. Genome-wide assessment of differential translations with ribosome profiling data. *Nat Commun* 2016;7:11194.
- [36] Goulet I, Gauvin G, Boisvenue S, et al. Alternative splicing yields protein arginine methyltransferase 1 isoforms with distinct activity, substrate specificity, and subcellular localization. *J Biol Chem* 2007;282(45):33009–21.
- [37] Tang J, Gary JD, Clarke S, et al. Prmt 3, a type i protein arginine n-methyltransferase that differs from prmt1 in its oligomerization, subcellular localization, substrate specificity, and regulation. *J Biol Chem* 1998;273:16935–45.
- [38] Frankel A, Clarke S. Prmt3 is a distinct member of the protein arginine n-methyltransferase family. Conferred of substrate specificity by a zinc-finger domain. *J Biol Chem* 2000;275:32974–82.
- [39] Saha K, Adhikary G, Eckert RL. Mep50/prmt5 reduces gene expression by histone arginine methylation and this is reversed by pkcdelta/p38delta signaling. *J Invest Dermatol* 2016;136:214–24.
- [40] Guderian G, Peter C, Wiesner J, et al. Riok1, a new interactor of protein arginine methyltransferase 5 (prmt5), competes with picln for binding and modulates prmt5 complex composition and substrate specificity. *J Biol Chem* 2011;286:1976–86.
- [41] Bedford MT, Clarke SG. Protein arginine methylation in mammals: Who, what, and why. *Mol Cell* 2009;33:1–13.
- [42] Thandapani P, O'Connor TR, Bailey T, et al. Defining the rgg/rg motif. *Mol Cell* 2013;50:613–23.
- [43] Cheng D, Côté J, Shaaban S, et al. The arginine methyltransferase carm1 regulates the coupling of transcription and mRNA processing. *Mol Cell* 2007;25:71–83.
- [44] Feng Y, Maity R, Whitelegge JP, et al. Mammalian protein arginine methyltransferase 7 (prmt7) specifically targets rxr sites in lysine- and arginine-rich regions. *J Biol Chem* 2013;288:37010–25.
- [45] Huang da W, Sherman BT, Lempicki RA. Bioinformatics enrichment tools: Paths toward the comprehensive functional analysis of large gene lists. *Nucl Acids Res* 2009; 37: 1–13..
- [46] Huang DW, Sherman BT, Lempicki RA. Systematic and integrative analysis of large gene lists using david bioinformatics resources. *Nat Protoc* 2009;4:44–57.
- [47] Matera AG, Wang Z. A day in the life of the spliceosome. *Nat Rev Mol Cell Biol* 2014;15:108–21.
- [48] Kuhn P, Chumanov R, Wang Y, et al. Automethylation of carm1 allows coupling of transcription and mRNA splicing. *Nucl Acids Res* 2011; 39: 2717–26..
- [49] Bezzi M, Teo SX, Muller J, et al. Regulation of constitutive and alternative splicing by prmt5 reveals role for mdm4 pre-mRNA in sensing defects in the spliceosomal machinery. *Genes Dev* 2013;27:1903–16.
- [50] Harrison MJ, Tang YH, Dowhan DH. Protein arginine methyltransferase 6 regulates multiple aspects of gene expression. *Nucleic Acids Res* 2010; 38: 2201–16..
- [51] Dowhan DH, Harrison MJ, Eriksson NA, et al. Protein arginine methyltransferase 6-dependent gene expression and splicing: Association with breast cancer outcomes. *Endocr Relat Cancer* 2012; 19: 509–26..
- [52] Mann M, Zou Y, Chen Y, et al. Pelp1 oncogenic functions involve alternative splicing via prmt6. *Mol Oncol* 2014; 8: 389–400..
- [53] Chang FN, Navickas IJ, Chang CN, et al. Methylation of ribosomal-proteins in hela-cells. *Arch Biochem Biophys* 1976;172:627–33.
- [54] Goldenberg CJ, Elceirí GL. Methylation of ribosomal-proteins in hela-cells. *Biochim Biophys Acta* 1977;479:220–34.
- [55] Kruiswijk T, Kunst A, Planta RJ, et al. Modification of yeast ribosomal proteins. Methylation. *Biochem J* 1978; 175: 221–5..
- [56] Polevoda B, Sherman F. Methylation of proteins involved in translation. *Mol Microbiol* 2007; 65: 590–606..
- [57] Shin H-S, Jang C-Y, Kim HD, et al. Arginine methylation of ribosomal protein s3 affects ribosome assembly. *Biochem Biophys Res Commun* 2009;385:273–8.
- [58] Ren J, Wang Y, Liang Y, et al. Methylation of ribosomal protein s10 by protein-arginine methyltransferase 5 regulates ribosome biogenesis. *J Biol Chem* 2010;285:12695–705.
- [59] Simsek D, Tiu GC, Flynn RA, et al. The mammalian ribo-interactome reveals ribosome functional diversity and heterogeneity. *Cell* 2017;169 (6):1051–1065.e18.
- [60] Choi S, Jung C-R, Kim J-Y, et al. Prmt3 inhibits ubiquitination of ribosomal protein s2 and together forms an active enzyme complex. *Biochim Biophys Acta* 2008;1780:1062–9.

- [61] Swiercz R, Person MD, Bedford MT. Ribosomal protein s2 is a substrate for mammalian Prmt3 (protein arginine methyltransferase 3). *Biochem J* 2005;386:85–91.
- [62] Swiercz R, Cheng D, Kim D, et al. Ribosomal protein rps2 is hypomethylated in Prmt3-deficient mice. *J Biol Chem* 2007;282(23):16917–23.
- [63] Tye BW, Commins N, Ryazanova LV, et al. Proteotoxicity from aberrant ribosome biogenesis compromises cell fitness. *eLife* 2019; 8: e43002..
- [64] Ingolia NT. Ribosome footprint profiling of translation throughout the genome. *Cell* 2016;165(1):22–33.
- [65] Boisvert F-M, Côté J, Boulanger M-C, et al. A proteomic analysis of arginine-methylated protein complexes. *Mol Cell Proteomics* 2003;2(12):1319–30.
- [66] Jeong H-J, Lee H-J, Vuong TA, et al. Prmt7 deficiency causes reduced skeletal muscle oxidative metabolism and age-related obesity. *Diabetes* 2016;65(7):1868–82.
- [67] Penney J, Seo J, Kritskiy O, et al. Loss of protein arginine methyltransferase 8 alters synapse composition and function, resulting in behavioral defects. *J Neurosci* 2017;37(36):8655–66.
- [68] Nicholson TB, Chen T, Richard S. The physiological and pathophysiological role of Prmt1-mediated protein arginine methylation. *Pharmacol Res* 2009;60:466–74.
- [69] Tee W-W, Pardo M, Theunissen TW, et al. Prmt5 is essential for early mouse development and acts in the cytoplasm to maintain es cell pluripotency. *Genes Dev* 2010;24:2772–7.
- [70] Pawlak MR, Scherer CA, Chen J, et al. Arginine N-methyltransferase 1 is required for early postimplantation mouse development, but cells deficient in the enzyme are viable. *Mol Cell Biol* 2000;20:4859–69.
- [71] Yadav N, Lee J, Kim J, et al. Specific protein methylation defects and gene expression perturbations in coactivator-associated arginine methyltransferase 1-deficient mice. *Proc Natl Acad Sci USA* 2003; 100: 6464–6468..
- [72] Emmott E, Jovanovic M, Slavov N. Ribosome stoichiometry: From form to function. *Trends Biochem Sci* 2019;44:95–109.
- [73] Genuth NR, Barna M. The discovery of ribosome heterogeneity and its implications for gene regulation and organismal life. *Mol Cell* 2018;71:364–74.
- [74] Chang B, Chen Y, Zhao Y, et al. Jmjd6 is a histone arginine demethylase. *Science* 2007;318:444–7.
- [75] Vagin VV, Wohlschlegel J, Qu J, et al. Proteomic analysis of murine piwi proteins reveals a role for arginine methylation in specifying interaction with tudor family members. *Genes Dev* 2009;23:1749–62.
- [76] Kirino Y, Vourekas A, Sayed N, et al. Arginine methylation of aubergine mediates tudor binding and germ plasm localization. *RNA* 2010;16:70–8.
- [77] Chen C, Nott TJ, Jin J, et al. Deciphering arginine methylation: Tudor tells the tale. *Nat Rev Mol Cell Biol* 2011;12:629–42.



Huan-Huan Wei received her Ph.D. degree from the South China Institute of Botany, Chinese Academy of Sciences (CAS). She worked in FuDan University as a lecturer after graduation and joined Zefeng Wang's group at CAS-MPG Partner Institute for Computational Biology (PICB) in 2016. She is an assistant professor at PICB, Shanghai Institute of Nutrition and Health, CAS. Her research interest focuses on the mechanisms and regulation of aberrant alternative splicing in cancers and the mechanisms and functions of arginine methylation on RNA splicing factors.



Zefeng Wang is a principal investigator and director of PICB, Shanghai Institute of Nutrition and Health, CAS. His research focuses on the regulation of gene expression in RNA level. He has made significant contribution to the field of RNA biology by developing a series of genomic approaches to study RNA splicing in a systematic fashion.